

MATHEMATICAL MODELING, COMPUTER SIMULATION, CONTROL AND APPLICATIONS OF A STABILIZED PLATFORM OF AN AIRBORNE SENSOR

M. Bäumker¹, F.-J. Heimes¹, H. Hahn², W. Klier², Rainer Brechtken¹ and Torsten Richter¹

¹University of Applied Sciences Bochum
Lennershofstrasse 140, D-44801 Bochum

²University of Kassel
Mönchebergstrasse 7, D-34109 Kassel

KEY WORDS: platform kinematics, nonlinear control, stabilization, airborne sensor orientation, georeferencing, INS/GPS

ABSTRACT

A high precision stabilized platform has been developed at the University of Applied Sciences Bochum - in cooperation with others. The platform is designed to carry different types of remote sensing devices. It is the goal that the system is able to provide precisely stabilized imagery even for low flying light aircrafts under turbulent air conditions. Residual image inclinations and yaw deviations are recorded. Together with the data of the (D)GPS augmented inertial navigation system (INS) the complete exterior orientation data are delivered. At the University of Kassel (Control Engineering and System Theory Group) detailed model equations in **DE**-form (**d**ifferential **e**quations) of the spatial motions of the stabilized platform have been developed. These model equations serve as basis for a **computer simulation** of the mechanism, for nonlinear and linear **controller design** and **model parameter identification** using test flight data. The computer simulation is used to investigate the influence of various control algorithms, filter algorithms, actuators and other components under various external and internal disturbances in order to find optimal solutions for a fast and precise stabilization of a remote sensing device (camera, scanner, video, etc.). A research airplane is available to measure in-flight data under different air conditions. By a comparison of actual in-flight data and simulation data, a detailed analysis of the system is carried out. The results of this research work are considered to be of basic importance for imaging systems to be operated under turbulent air conditions (e.g. light aircraft flying low). To produce optimal coverage with a scanning system or with a digital video system is of crucial importance. Of course it is possible to georeference imagery on the basis of INS/DGPS if there is non-perfect or even no stabilization, but gaps may occur depending on the degree of angular motions of the airplane. This research work enables to find an optimal design and to determine the limiting factors of the mechanism considered. In addition, the suitability of using an autopilot for precise survey flight is going to be investigated.

1 INTRODUCTION

Since the Global Positioning System (GPS) is fully operational it has been established as a standard guidance and navigation system for numerous applications on aircrafts, land vehicles and ships. Considerable improvements with respect to the standard positioning service of the GPS based upon C/A code receivers can be achieved by applying the *differential* GPS technique (DGPS) or the latest milestone: the *ambiguity resolution on the fly* (OTF). All GPS methods are suffering under the loss of the satellite signals due to obstacles and manoeuvres of the vehicle, or other disturbances that are influencing the successful application of the OTF method. Further on high precision navigation applications, especially for remote sensing applications, require accurate lever arm corrections to transfer the position of the antenna phase centre to the desired site. But lever arm corrections depend on the availability of attitude (roll, pitch) and heading of the vehicle which cannot be delivered by the GPS. If the velocity vectors have to be transformed, additional rates are needed. For remote sensing applications without ground control the angles phi, omega and kappa are additionally required. Further on, to get perfect images a **stabilized platform for the sensor is needed**. All of these requirements can be ideally solved with a (D)GPS augmented inertial navigation system delivering all data needed to control a stabilized platform with camera and a flight management system for aircraft guidance and shutter release. Mathematical modeling and computer simulation will allow to find the best possible solutions for electronic control of the stabilized platform under various disturbances and to obtain precise stabilization even for light aircraft flying under turbulent air conditions.

2 THE NEW SYSTEM CONCEPT

Since several years a lot of effort has been spent at the Fachhochschule Bochum (in cooperation with the UC -Umweltconsulting) to develop an aerial survey system on the basis of small format aerial photography (Heimes et al. 1994, 1997). The basic configuration of a first prototype system consisted of a GPS receiver, stabilized mount and a notebook computer. The aircraft's attitude data for camera stabilization were derived from standard gyro instruments (vertical artificial horizon

gyro and directional gyro) with synchro outputs. The converted digital signals were used as inputs for the control loops. The practical trials showed that the stabilization was too slow due to the signal processing and that the performance of the cardanic type of mount was not satisfactory. Therefore, a completely new system was developed; the mechanical components (sensor mount) were constructed and built in cooperation with the University of Applied Sciences Cologne (Prof. Dr.-Ing. H. Gartung) and the company IBF (Ingenieurbüro Freudenberg). As a further consequence an inertial measurement unit (IMU) was chosen to have a better attitude reference. A disadvantage still was that the IMU was mounted beside the controlled camera platform on the bottom of the fuselage of the aircraft. Recently a new state of the art inertial measurement unit (IMU) has been selected which is now directly mounted on the camera and fixed to it. The new high performance system is especially designed for light aircrafts. Different medium- and small-format cameras or other remote sensing sensors can be used. At present adapters for the Rollei 6006 metric camera, the Contax RTS III (with film flattening and fiducial marks) and for the digital cameras Kodak DCS 420/DCS 460 are available. The latter one allows the direct production of digital orthophotos of local areas. The new system (see 1) consists of following components:

- a standard strapdown attitude and heading reference system from LITEF (Freiburg, Germany) with three fibre optical gyros (FOG)
- a 12 channel single frequency C/A-Code GPS receiver LEICA 9400 used as reference station
- a 12 channel single frequency C/A-Code GPS receiver LEICA 9400 used as rover
- a data link (telemetry, 433 Mhz, at least 1200 Bd)
- a processing unit (486 PC) with a multiple serial and digital IO-card (RS422, RS232)
- a mount control unit
- a stabilized sensor platform with camera and alignment fixture for the inertial measurement unit
- a flight management system (FMS)
- a digital camera, e.g. Kodak DCS420 or Kodak DCS460

The LITEF strapdown shown in Figure 2(a) includes three fibre optical gyros (FOG) with a fiber length of 500 m and three pendulum accelerometers and is directly and firmly mounted on the camera (Figure 2(b)). Their typical accuracies are listed in Table 1. The original 64 Hz inertial measurements (rates and accelerations) are acquired via a RS422 interface by the processing unit and then combined in a Kalman Filter with the measurements of a (D)GPS using two single frequency C/A code receivers LEICA 9400 as reference and rover. To use the raw data of the reference receiver in the optional DGPS mode additionally a standard data link is required. The synchronization of the inertial and GPS data is managed with the help of the PPS-signal of the rover receiver and an internal clock.

	gyro	accelerometer
Drift / bias	0.1°/h	0.5 mg
scale factor error	100 ppm	1000 ppm
noise	0.02°/√h	10μg

Table 1: Accuracies of the inertial sensors

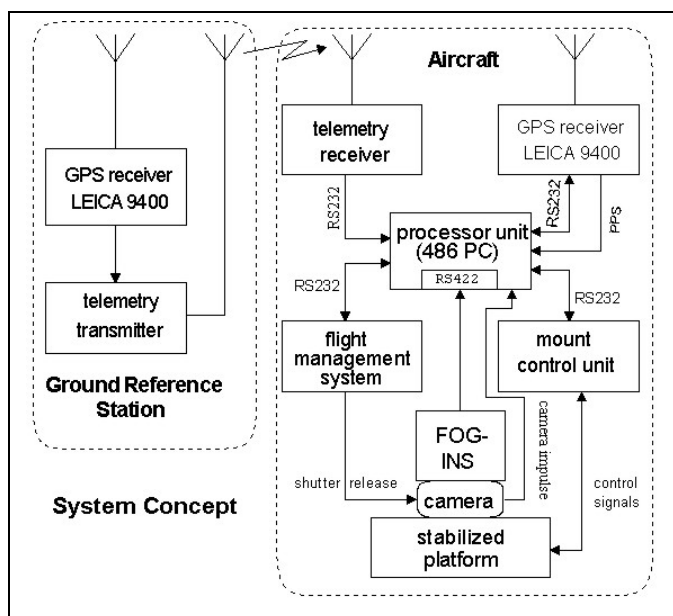
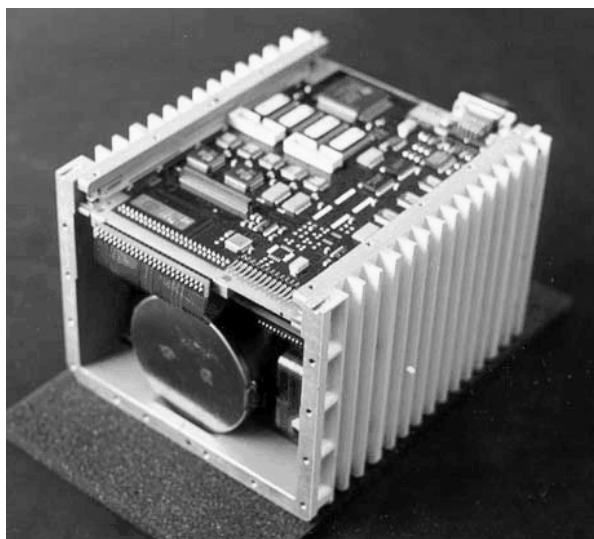


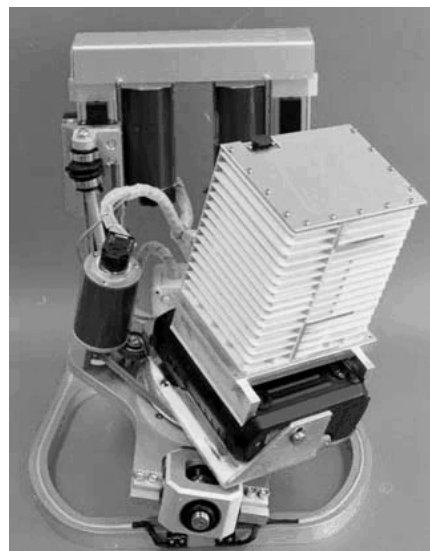
Figure 1: Components of the hybrid system

The system is able to perform a self alignment within two minutes and can bridge GPS data gaps during several minutes. In the GPS augmented mode position accuracies of 0.3 m can be achieved. Roll and pitch angles are measured with an accuracy of 0.02° and heading with 0.05°. Details of the system, its mechanization and the applied Kalman Filter are given in (Bäumker 1995a,b). The processing unit (PC) calculates and outputs with a frequency of 64 Hz all the data (position, velocity, attitude angles, heading, track angle, body rates, body accelerations) which are required to drive the flight management system and to control the stabilized sensor platform by the mount control unit. The flight management system is responsible for the shutter release of the camera and delivers the flight line information for the display of the pilot. The mount control unit controls the stabilized sensor platform and determines the control residuals (inclination and yaw deviation) which are fed back to the processing unit. In case of the shutter release the instant residuals are stored together with the actual position, velocity, rates, heading, roll and pitch angles on the hard disk of the processing unit. The stabilized platform Figure 2(b) consists of a stable three-point suspension and three highly dynamic servo motors. Angular motions of the aircraft measured by the inertial measurement unit and the calculated attitude and heading angles are processed by the mount control unit to stabilize the platform on which the camera and the IMU are mounted. This stabilization ensures perfect images for numerous applications even for low flying light aircrafts under turbulent conditions. Another

advantage is that the exterior orientation elements of each image (position and angles!) are directly measured by the INS/GPS system. Due to the continuous feedback of the control residuals and of the shutter release signal of the camera to the processor unit the complete exterior orientation data are immediately present at the time of exposure without any ground control.



(a) Inertial measurement unit (IMU) from LITEF with the coil of one of the three fibre optical gyros



(b) Stabilized Platform, the IMU mounted on the top of the digital camera Kodak DCS460

Figure 2: Photos of inertial unit (IMU) from LITEF and of stabilized platform

3 MATHEMATICAL MODELING AND CONTROL DESIGN OF A STABILIZED PLATFORM

In this section a mathematical model of spatial motions of the platform–airplane–system (cf. Figures 2(b) and 4) will be derived, compare (Hahn and Klier, 1999). This theoretical model serves as a basis for **experimental identification of model parameters, computer simulations and controller design** of this mechanism. To set up and run computer simulations of the mechanism and to check its functioning, correctness and efficiency, a **nonlinear kinematic decoupling controller** together with a **standard linear actuator controller** and a **nonlinear mapping** of various **measured global coordinates** will be included in the modeling process. The total control system considered is shown in Figure 3. The nonlinear kinematic decoupling controller will be derived from **kinematic relations** of the massless links (cf. Figure 4). The nonlinear mapping of measured signals includes additionally to the **kinematic relations** of the massless links a single equation of the **kinematic constraint position equations** of the **universal joint** between platform and airplane (cf. Figure 4). These relations will be derived and collected in **Section 3.1**. In **Section 3.2** the model equations of the spatial behavior of this system will be represented in form of differential equations (**DE**) that are well suited both, for **computer simulations** using standard integration techniques, and for standard **linear and nonlinear controller design**.

3.1 Kinematics

In this section kinematic relations will be derived including the **universal joint** and **two massless links** between platform and airplane (cf. Figures 4(a) and 4(b)).

3.1.1 Constraint kinematic relations

The **constraint kinematic position equations** of the **universal joint** are defined by the relations

$$g^k(p) = \begin{bmatrix} g_1^k(p_1, p_2) \\ g_2^k(\eta_1, \eta_2) \end{bmatrix} := \begin{bmatrix} r_{P_1O}^R - r_{P_2O}^R + A^{RL_1} \cdot r_{QP_1}^{L_1} - A^{RL_2} \cdot r_{QP_2}^{L_2} \\ p_r^T(x) \{ A^{Q_1L_1} \cdot A^{L_1R} \cdot A^{RL_2} \cdot A^{L_2Q_2} \} p_r(y) \end{bmatrix} = \begin{bmatrix} 0_3 \\ 0_1 \end{bmatrix} \text{ with} \quad (1a)$$

$$\eta_1 := [\phi_1, \theta_1, \psi_1]^T \text{ (Bryant angles of the airplane)} , \quad \eta_2 := [\phi_2, \theta_2, \psi_2]^T \text{ (Bryant angles of the platform)} , \quad (1b)$$

$$A^{LQ_iL_i} := A^{Q_iL_i} , \quad LQ_i = [e_{xQ_i}, e_{yQ_i}, e_{zQ_i}] \text{ (unit vectors of frame } LQ_i) , \quad A^{LQ_iL_i} := I_3 , \quad i = 1, 2 \quad (1c)$$

with transformation matrices

$$A^{RL_i} := \begin{bmatrix} \cos \theta_i \cdot \cos \psi_i & -\cos \theta_i \cdot \sin \psi_i & \sin \theta_i \\ \cos \phi_i \cdot \sin \psi_i + \sin \phi_i \cdot \sin \theta_i \cdot \cos \psi_i & \cos \phi_i \cdot \cos \psi_i - \sin \phi_i \cdot \sin \theta_i \cdot \sin \psi_i & -\sin \phi_i \cdot \cos \theta_i \\ \sin \phi_i \cdot \sin \psi_i - \cos \phi_i \cdot \sin \theta_i \cdot \cos \psi_i & \sin \phi_i \cdot \cos \psi_i + \cos \phi_i \cdot \sin \theta_i \cdot \sin \psi_i & \cos \phi_i \cdot \cos \theta_i \end{bmatrix}, \quad i = 1, 2 \quad (1d)$$

and projection vectors $p_r(x) := [1, 0, 0]^T$, $p_r(y) := [0, 1, 0]^T$. The constraint kinematic relation (1a) has been obtained from suitable **projections of the vector loop** and **orientation loop equations** of the mechanism, including the universal joint (point Q of Figures 4(a) and 4(b)), compare (Hahn, 1997).

3.1.2 Actuator kinematic relations and nonlinear kinematic decoupling controller

The **kinematic relations** of the two massless links that (in addition to the universal joint) connect the platform to the airplane, are briefly derived from appropriate vector loop equations (cf. Figure 4(b)). These relations will be called **partial kinematic relations** as they do not include the kinematics of the universal joint (1a). The resulting **kinematic**

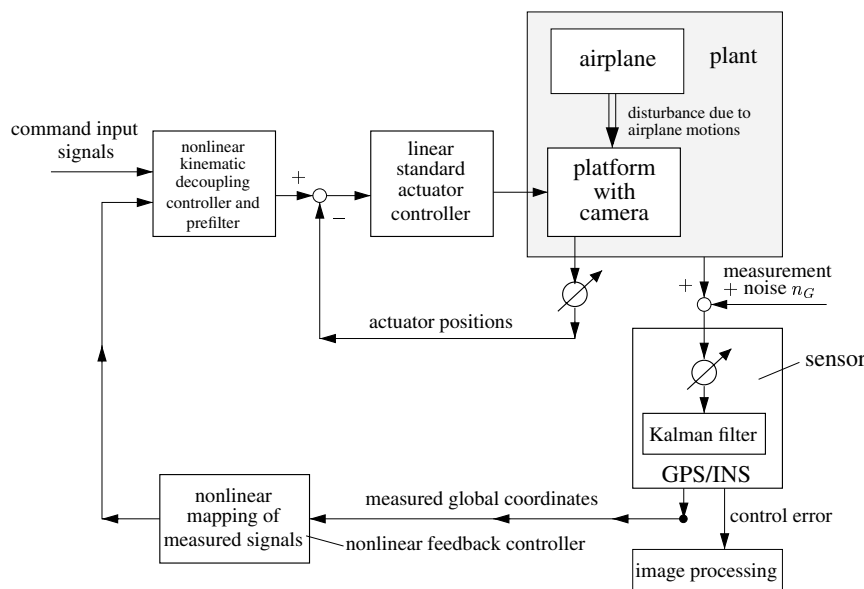


Figure 3: Control system including the plant model, a linear actuator controller, a nonlinear kinematic decoupling controller and a nonlinear algorithm for processing of measured signals

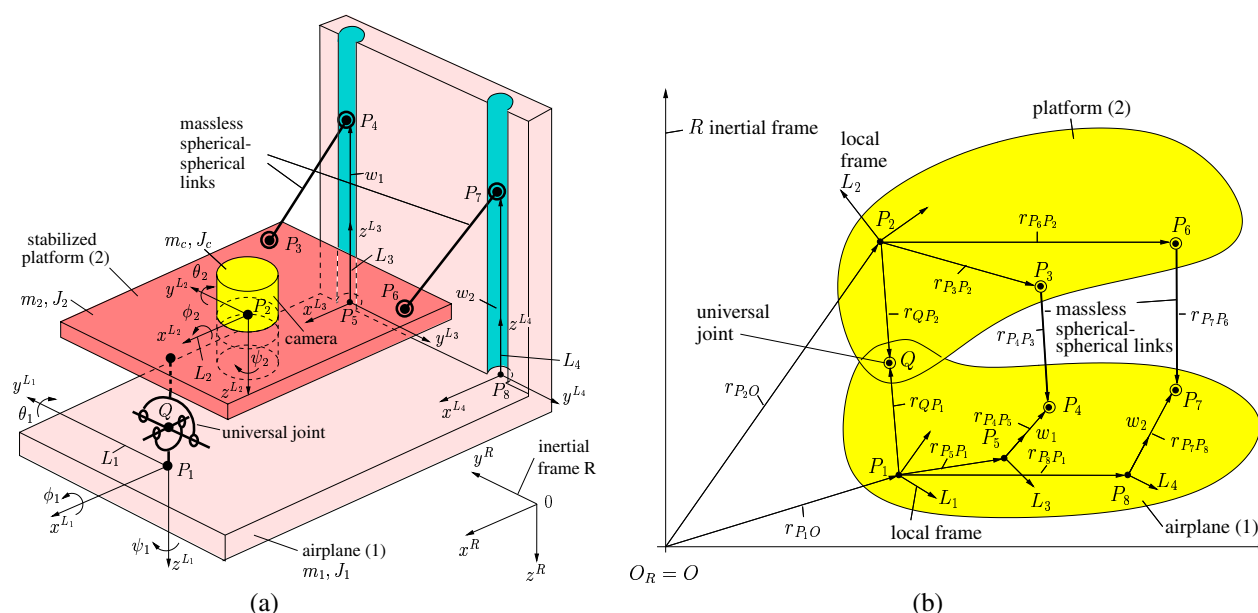


Figure 4: Drawing (Figure (a)) and Vector diagrams (Figure (b)) of the platform for deriving kinematic relations

relations of the massless spherical–spherical links (partial platform kinematics) are

$$g(\eta_1, \eta_2, w) := [g_1(\eta_1, \eta_2, w_1), g_2(\eta_1, \eta_2, w_2)]^T = 0 \quad \text{with} \quad (2)$$

$$g_i(\eta_1, \eta_2, w_i) := \left\{ \left[A^{RL_1} \cdot A^{L_1 L_{i+2}} \cdot r_{P_{3 \cdot i+1} P_{3 \cdot i+2}}^{L_{i+2}} + A^{RL_1} \cdot r_{P_{3 \cdot i+1} Q}^{L_1} - A^{RL_2} \cdot r_{P_{3 \cdot i} Q}^{L_2} \right]^T \cdot \left[A^{RL_1} \cdot A^{L_1 L_{i+2}} \cdot r_{P_{3 \cdot i+1} P_{3 \cdot i+2}}^{L_{i+2}} + A^{RL_1} \cdot r_{P_{3 \cdot i+2} Q}^{L_1} - A^{RL_2} \cdot r_{P_{3 \cdot i} Q}^{L_2} \right] \right\}^{1/2} - l \equiv 0, \quad i = 1, 2, \quad (3)$$

$$A^{L_1 L_{i+2}} := \begin{bmatrix} 1, & 0, & 0 \\ 0, & -1, & 0 \\ 0, & 0, & -1 \end{bmatrix}, \quad r_{P_{3 \cdot i+1} P_{3 \cdot i+2}}^{L_3} := \begin{bmatrix} 0 \\ 0 \\ w_i \end{bmatrix}^T \quad \text{(actuator displacements)}, \quad i = 1, 2 \quad (4)$$

and with the length of each massless link $l := |r_{P_3 P_4}^R| = |r_{P_6 P_7}^R|$. The solution of the partial platform kinematics (2) with respect to w assuming positive actuator displacements w_i is

$$w = \begin{bmatrix} w_1 \\ w_2 \end{bmatrix} = t_p(\eta_1, \eta_2) = \begin{bmatrix} t_{p_1}(\eta_1, \eta_2) \\ t_{p_2}(\eta_1, \eta_2) \end{bmatrix} = \begin{bmatrix} -\frac{a_{11}(\eta_1, \eta_2)}{2} + \frac{\sqrt{a_{11}^2(\eta_1, \eta_2) - 4 \cdot a_{10}(\eta_1, \eta_2)}}{2} \\ -\frac{a_{21}(\eta_1, \eta_2)}{2} + \frac{\sqrt{a_{21}^2(\eta_1, \eta_2) - 4 \cdot a_{20}(\eta_1, \eta_2)}}{2} \end{bmatrix}. \quad (5)$$

These expressions will be called **actuator kinematics**. The coefficients a_{10} , a_{11} , a_{20} and a_{21} in (5) include lengthy and complex expressions and are omitted here. They were computed using the computer algebra system MACSYMA.

The control task is to keep the platform orientation parallel to the inertial frame R ($\phi_{2d} = \theta_{2d} = 0$) with an arbitrary chosen yaw angle of the airplane ($\psi_{2d} = \psi_1$). Replacing in the **actuator kinematics relations** (5) the orientation variables of the platform ϕ_2 , θ_2 , ψ_2 by desired orientation variables of the platform ϕ_{2d} , θ_{2d} , ψ_{2d} , i.e. inserting

$$\phi_2 = \phi_{2d} \stackrel{!}{=} 0, \quad \theta_2 = \theta_{2d} \stackrel{!}{=} 0, \quad \psi_2 = \psi_{2d} \stackrel{!}{=} \psi_1 \quad \text{or} \quad \eta_2 = \eta_{2d} \quad \text{and} \quad w_d := w \quad \text{(desired actuator positions)} \quad (6)$$

into (5) with $w_d = (w_{1d}, w_{2d})^T$ as resulting desired displacements of the drives and with $\psi_{2d} = \psi_2 = \psi_1$ as assumed (desired) common orientation angle of the platform and airplane provides the nonlinear relations

$$w_d = t_p(\eta_1, \eta_{2d}) \quad \text{with} \quad \eta_{2d} := [0, 0, \psi_1]^T, \quad (7)$$

that serve as **nonlinear decoupling controller** and **prefilter** of the plant (**platform** together with the **camera**, disturbed by the **airplane**). They are too lengthy to be explicitly listed here.

3.1.3 Signal processing kinematic relations

The solutions $\eta_1 \in \mathbb{R}^3$ or $\eta_2 \in \mathbb{R}^3$ of the nonlinear system equations (3), (1a) or (8)

$$\bar{g}(\eta_1, \eta_2, w) := \begin{bmatrix} g_1(\eta_1, \eta_2, w_1) = 0 \\ g_2(\eta_1, \eta_2, w_2) = 0 \\ g_2^k(\eta_1, \eta_2) = 0 \end{bmatrix}, \quad \text{written in the form} \quad (8)$$

$$\eta_1 = h_1(\eta_2, w) := \text{sol}_{\eta_1}(\bar{g}(\eta_1, \eta_2, w) = 0) \quad (9a) \quad \text{and} \quad \eta_2 = h_2(\eta_1, w) := \text{sol}_{\eta_2}(\bar{g}(\eta_1, \eta_2, w) = 0) \quad (9b)$$

are called **signal processing kinematics**. Contrary to the actuator kinematic relations (5), the **kinematic relations** (9a) and (9b) additionally include an equation of the **kinematic constraint position equations** of the **universal joint**. They can only be **computed numerically**. The solution of the **signal processing kinematics** (9a) is used as **nonlinear mapping of measured global variables** η_2 and can be interpreted as **nonlinear feedback controller** in the control loops of Figure 3. The solution of **signal processing kinematics** (9b) is used as **image processing block** in the control loop of Figure 3. The kinematic relations (9a) and (9b) will also be used as parts of **computed torque control algorithms** and of **exact linearization controllers**. These control algorithms will be presented in an additional paper investigating different control strategies of the platform stabilization.

3.2 Differential equations of motion (DE)

The differential equations of motion of the platform have been derived in several steps (compare (Hahn and Klier, 1999)):

Step 1: Derivation of differential–algebraic equations (**DAE**) including

- **spatial equations of motion** of two unconstrained rigid bodies (**airplane** and **platform/camera**),
- **kinematic differential equations** between angular velocities and derivatives of orientation angles (Bryant angles) of the two rigid bodies,

- **models** of the **drives** of the platform,
- **kinematic constraint** position, velocity and acceleration **equations** of the **universal joint** (1a), and
- **active constraints** of the **airplane**, derived on the assumption that the airplane position $r_{P_{10}}^R = (x_{P_{10}}^R, y_{P_{10}}^R, z_{P_{10}}^R)^T$ and η_1 , velocity $\dot{r}_{P_{10}}^R$ and $\omega_{L_1 R}^{L_1} = (\omega_{x_1}^{L_1}, \omega_{y_1}^{L_1}, \omega_{z_1}^{L_1})^T$, and acceleration $\ddot{r}_{P_{10}}^R$ and $\dot{\omega}_{L_1 R}^{L_1}$ are currently measured. They can be replaced by the **measured** position variables $r_{P_{10m}}^R$ and η_{1m} , by the **measured** velocity variables $\dot{r}_{P_{10m}}^R$ and $\omega_{L_1 Rm}^{L_1}$, and by the **measured** acceleration variables $\ddot{r}_{P_{10m}}^R$ and $\dot{\omega}_{L_1 Rm}^{L_1}$, respectively. Then the motion of the platform can be considered as being **constrained** by the airplane motion. This implies the **active constraint position equation**

$$g^a(p) := \begin{bmatrix} r_{P_{10}}^R - r_{P_{10m}}^R \\ \eta_1 - \eta_{1m} \end{bmatrix} \quad (10)$$

together with the associated **active constraint velocity and acceleration equations**.

Step 2: Symbolic **computation** of **dependent coordinates** as functions of the independent coordinates $p_0 := (\phi_2, \theta_2)^T$ and $v_0 := (\omega_x^{L_2}, \omega_y^{L_2})^T$.

Step 3: Symbolic **computation** of **Lagrange multipliers** as functions of the independent coordinates p_0 and v_0 .

Step 4: **Elimination** of the **dependent coordinates** and **Lagrange multipliers**.

Step 5: **Rearrangement** and physical **interpretation** of the final model equations.

The above steps yield the **differential equations of motion (DE)**

$$M_0(p_0, \psi_{1m}) \cdot \dot{v}_0 = q_{G_0}(p_0, \psi_{1m}, v_0, \omega_{L_1 Rm}^{L_1}) + q_{D_0}(p_0, \eta_{1m}, v_0, \omega_{L_1 Rm}^{L_1}) + q_Z(p_0, \eta_{1m}, \ddot{r}_{P_{10m}}^R, \omega_{L_1 Rm}^{L_1}, \dot{\omega}_{L_1 Rm}^{L_1}) + q_M(p_0, \eta_{1m}, v_0, \omega_{L_1 Rm}^{L_1}) + J_{\phi\theta}^T(p_0, \eta_{1m}) \cdot F_A \quad (11)$$

with the generalized mass matrix $M_0 \in \mathbb{R}^{2,2}$, the vector of gyroscopic terms $q_{G_0} \in \mathbb{R}^2$, the vector of damping terms $q_{D_0} \in \mathbb{R}^2$, the vector of disturbance terms (due to airplane motion) $q_Z \in \mathbb{R}^2$, the vector of mixed (airplane and platform) terms $q_M \in \mathbb{R}^2$, the vector of actuator forces $F_A := K_A \cdot u_A$ with $u_A \in \mathbb{R}^2$ as vector of actuator input voltages and the diagonal matrix $K_A \in \mathbb{R}^{2,2}$ of the actuator gain factors, and with the transformation matrix $J_{\phi\theta}^T \in \mathbb{R}^{2,2}$ that maps the actuator forces $F_A = [F_{A_1}, F_{A_2}]^T$ into torques with respect to x^{L_2} and y^{L_2} as rotation axes (cf. Figure 4(a)).

4 COMPUTER SIMULATIONS

In this section some preliminary computer simulation results are presented using measured airplane signals of standard test flights. Figure 5 shows computer simulation results obtained for the platform (11) including ideal actuator models, the **nonlinear kinematic decoupling controller** (7) and a **linear standard actuator controller** $u_A = K_P \cdot (w - w_d)$ (cf. Block diagram 3). These results show that the **nonlinear kinematic decoupling controller** (7) together with the **standard actuator controller** provide an **acceptable transient behavior** in the degrees of freedom of the platform (ϕ_2, θ_2) for the desired orientation of the platform ($\phi_{2d} \equiv \theta_{2d} \equiv 0$), an **acceptable decoupling behavior** of the degrees of freedom of the platform, and a **good disturbance rejection behavior**. The design of more **efficient and sophisticated linear and nonlinear controllers** and results obtained by these controllers, both, in computer simulations with realistic actuator models and in flight experiments, will be presented in another paper.

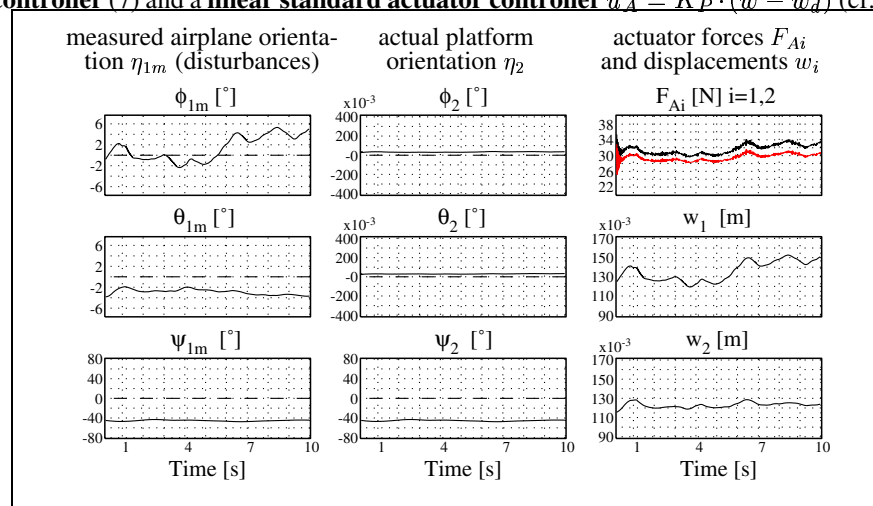


Figure 5: Computer simulation results for desired horizontal orientation of the platform ($\phi_{2d} \equiv \theta_{2d} \equiv 0$)

5 APPLICATIONS OF THE SYSTEM

5.1 Performance considerations for direct georeferencing without ground control

The system's main potentials are to be seen in the fact that it allows to produce precisely stabilized and directly georeferenced imagery. From this imagery DEM's (Digital Elevation Models) may be derived for producing digital orthophotos;

besides this it is possible to carry out 3D data capturing for photogrammetric mapping resp. for GIS, facility management and for all different types of monitoring (coastal zones, forestry, vegetation, power lines, pipe lines, etc.). All this may be done without determining ground control points in the terrain.

Three accuracy classes are to be considered:

a) With aerial triangulation

Aerial triangulation (without ground control) based on the parameters of exterior orientation as determined in-flight is carried out before data capturing. Of course final accuracy (especially rel. accuracy) depends very much on image scale. But for large to medium image scales the limiting factor is the positioning accuracy of the perspective centres.

For object points the following absolute accuracy is typical: $\sigma_{x,y} = 0.30$ m. This is to be obtained for block configuration as well as for strips. The accuracy in height is depending on the base to height ratio.

b) No aerial triangulation but accurate in-flight system calibration

(s. Dr. Jacobson, University Hannover, ASPRS Annual Convention, Washington 2000) Here data capturing is carried out directly from the images on the basis of the parameters of exterior orientation as determined in-flight. A test area (reference area) with a few control points (e.g. 8 points) is to be available. Before starting a project and after finishing aerial images have to be taken of this test area. With these images a bundle adjustment with self calibration is carried out to be able to correct for actual image distortion and to derive angular off-sets ("misalignments") between INS reference and image coordinate system and to correct also for systematic errors in positioning. For object points the following absolute accuracy is typical: $\sigma_{x,y} = 0.50$ m.

The accuracy in height is depending on the base to height ratio.

c) No aerial triangulation, accurate laboratory calibration

The inner orientation as well as the angular off-sets between INS reference and image coordinate system may also be derived from laboratory calibration. At the University of Applied Sciences Bochum a test field has been established (Diploma Work Mrs. Wippermann and Mr. Willkom) for complete system calibration. Ca 50 points have been signaled (coded bar marks, according to Ir. R. Kroon, Geodelta, Delft, Netherlands).

Some points have been determined in WGS 84 (Gauss-Krueger-Projection) as control points. In simulated aerial survey flight the ca 30 m long and ca 10 m wide test field has been photographed with the UMK 10/1318 metric camera. In a bundle adjustment all points could be determined with an accuracy better than 1 mm. The test field is three-dimensional ("flight height" between 7 m and 3.5 m above ground) to be able to determine also the principal distance with very good accuracy. With the coded bar marks it is the goal to do the image coordinate measurements for future system calibrations in an automatic way. Experience has to be collected to see how constant the system calibration parameters will remain with time. For object points an absolute accuracies is expected in the order of: $\sigma_{x,y} = 0.50$ m up to 1.50 m. The accuracy in height again is depending on the base to height ratio.

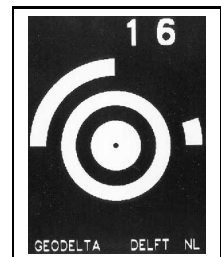


Figure 6: Coded bar marks as control points for complete system calibration

5.2 Pilot Project: Road Data Base

In September 1998 the system was installed in a survey aircraft of Hansa Luftbild - German Air Survey. In a pilot project for setting up a road data base aerial image data were collected for 80 large road intersections. The camera used was the digital camera Kodak DCS-460 (appr. 2000 x 3000 pixels). At a flight height of 840 m and with a focal length of 24 mm this resulted in a photo scale of 1:35.000. Many intersections could be covered by only one stereo model. For most of the intersections three up to six images were to be taken. But with the Kodak DCS-460 only the first two images of a series can be taken with a short time interval, after that the time interval between two images is appr. 8 seconds. Because of this fact most of the short flight lines had to be flown twice. Figure 8 shows the complete flight track. Of course the survey navigation and camera release were performed by means of computer supported flight management.



Figure 7: System Installed in a Survey Aircraft of Hansa Luftbild - German Air Survey

For this project it was specified to produce digital orthophotos per road intersection as well as vector data (axis of roads and road lanes). The required accuracy was $\sigma_{x,y} = 1.00$ m. Within this pilot project there were existing topographic

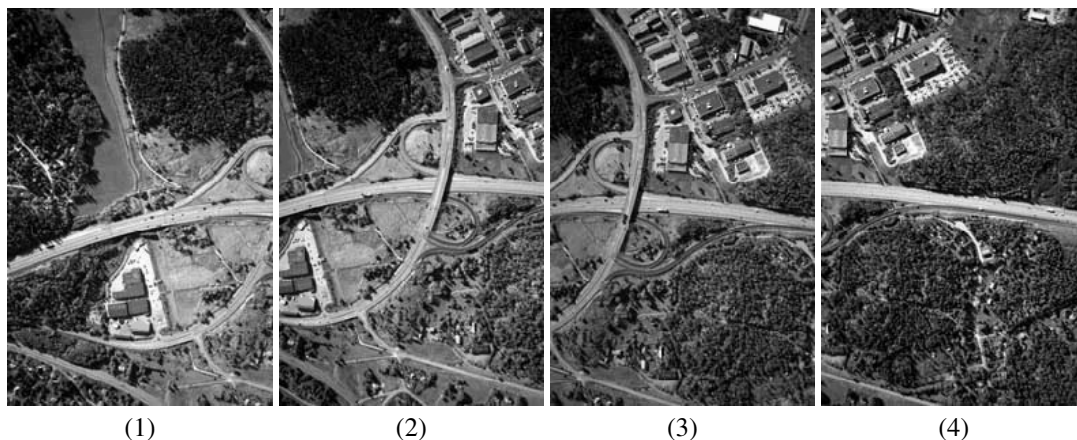
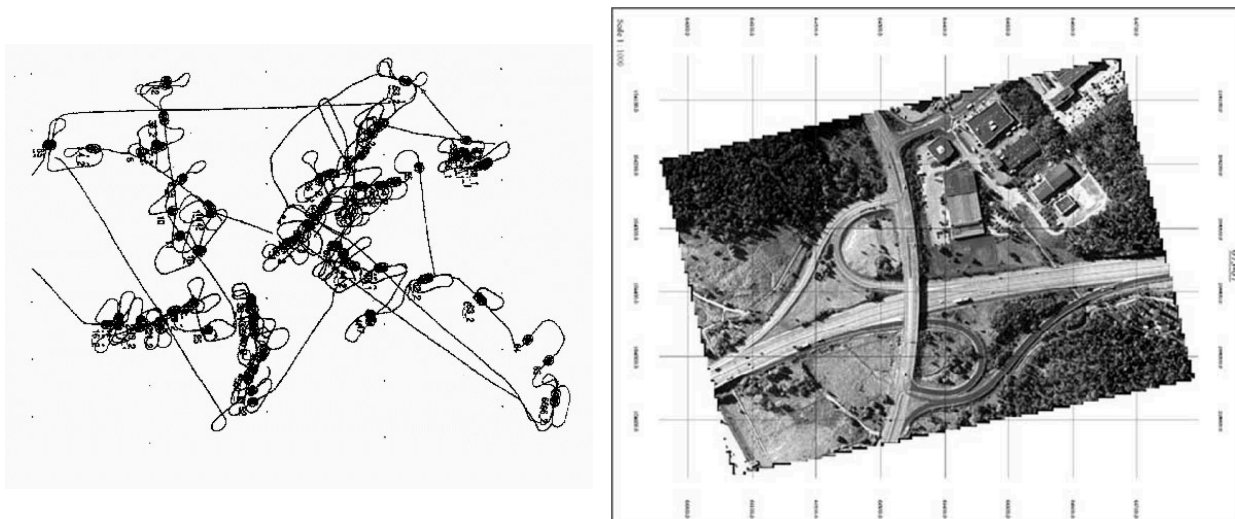


Figure 8: Images Taken with the Digital Camera KODAK DCS-460 (appr. 2000 x 3000 Pixels), Flight Height = 840 m, Focal Length = 24 mm, Image Scale = 1:35.000. Two up to six images were to be taken per road intersection.

maps in scale 1:1.000. From these maps ground control points could be obtained for the purpose of orientation of images. For the future it is intended to carry out the photogrammetric work without any control point: **Direct Georeferencing without Ground Control!** With the new system set-up (INS fixed to the camera) the performance requirement can be fulfilled. Accurate in-flight system calibration is needed according to chapter 5.1 b.



(a) Complete Flight Track to Take Digital Images of 80 Road Intersections. Most of the Intersections had to be Flown twice because of the Problem of Time Intervall between two Images.

(b) Digital Orthophoto of one Road Intersection with Superimposed Vector Data(Road Axis and Axis of Road Lanes).

Figure 9: Complete flight track and digital orthophoto of one road intersection

5.3 New applications

a) Direct orthophotos in combination with laser scanning

Laser scanning is applied to determine DEM's for different applications, e.g. for road planning, for power line monitoring etc. In addition to DEM data in many cases digital orthophotos are needed. With the system described digital orthophotos may be produced in two different but most efficient ways:

–On the basis of the DEM digital orthophotos may be derived from small format aerial photography (or digital aerial images) taken synchronously with the laser scanning. The focal length of the camera may be adapted in such a way that the same strip width is obtained as with laser scanning. No ground control points are needed because the elements of exterior orientation are determined in-flight.

–In case of only moderate accuracy requirements the digital orthophotos may be produced by applying a digital line camera with a somewhat longer focal length. Because of the high performance stabilization the output of the digital line camera is an orthophoto (slight image displacement within lines may be negligible).

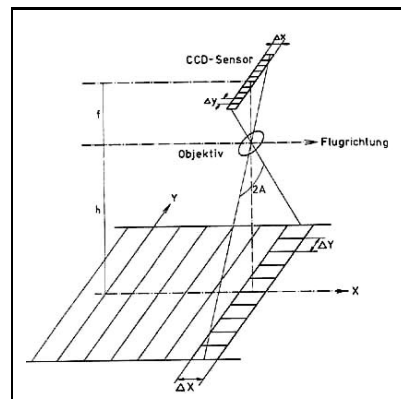


Figure 10: Long Focus Digital Line Camera

b) Digital video

Digital video may be very useful for different types of aerial monitoring (e.g. pipe line or power line monitoring). Even taken from light aircraft under turbulent air conditions the video images are stabilized with very high performance. In addition the elements of exterior orientation are determined for each video image. This means that 3D-object-measurements may be taken at any spot covered by the images. These measurements may be done stereoscopically or monoscopically (with automatic correlation of second image or image sequence, in this field a cooperation exists with Geodelta, Delft, and Prof. Ir. N. Mulder, TU Twente, Enschede, Netherlands).

6 CONCLUSIONS

The lighter the aircraft (and the lower the flight height) the higher the requirements on the stabilization of the photogrammetric camera or other remote sensing devices. To fulfil these requirements a stabilized platform has been developed and improved in the last years at the University of Applied Sciences Bochum. The system consists of a stable three-point servo-driven mount controlled by the data of a (D)GPS augmented Inertial Navigation System (INS from LITEF). The GPS receivers used as reference and rover are the single frequency receivers LEICA 9400 providing a position accuracy of appr. 0.3 m. Besides the position the system delivers the ϕ_2 , θ_2 and ψ_2 angles which are derived from the measurements of the INS and the control residuals (inclinations and yaw deviations). Thus the **system provides stabilized and fully georeferenced imagery** – elements of exterior orientation are determined in-flight. A detailed mathematical model of the stabilizing system in form of differential equations (DE's) has been developed at the University of Kassel (Control Engineering and System Theory Group). These model equations have been used as basis for computer simulations of the system and will serve as basis for model parameter identification and controller design in further investigations. The computer simulation enables to investigate the influence of various control algorithms, filter algorithms, actuators and other components under various external and internal disturbances, in order to find optimal solutions for a fast and precise stabilization of a remote sensing device (camera, scanner, video, etc.). A research airplane is available to measure in-flight data under different air conditions. By a comparison of actual in-flight data and simulation data, detailed analysis of the system is carried out. To produce optimal coverage with a scanning system or with a digital video system is of direct practical importance. Of course it is possible to georeference imagery on the basis of INS/DGPS if there is non-perfect or even no stabilization, but gaps may occur depending on the degree of angular motions of the airplane. This research work enables to find an optimal design and to determine the limiting factors of the mechanism considered. The perfect images allow aerial monitoring (biodiversity-, forest-clear-cut-, afforestation-, coastal-, soilerosion-, natural-disaster-, and other monitoring applications) without ground control. Further on the system is well suited for local surveys with medium format cameras and digital cameras (e.g. Kodak DCS-460).

REFERENCES

- M. Bäumker, December 1995a. DGPS-gestütztes Fahrzeugnavigationssystem mit faseroptischen Kreiseln, *Journal for Satellite-Based Positioning, Navigation and Communication*, Vol. 4/95, pp. 120-128.
- M. Bäumker, December 1995b. Basiswissen Inertial- und Sensortechnik, *Journal for Satellite-Based Positioning, Navigation and Communication*, Vol. 4/95, pp. 147-152.
- Heimes, Bäumker, Brechtken, Richter, August 1994. Photogrammetric Data Acquisition from Light Aircraft on the Basis of the High performance Camera Contax RTS III, *GIM*, 8/94 pp. 50 - 53.
- Graham, Read, Warner, 1996. *Small Format Aerial Photography*, Whittles Publishing, Caithness.
- Graham, 1997. *Digital Imaging*, Whittless Publishing, Caithness.
- Hahn, H., 1997. *Mathematical modeling of elementary rigid body mechanisms*, Vol. I and Vol. II. Universität-Gh Kassel, Fachgebiet Regelungstechnik und Systemdynamik (Maschinenbau), Lecture Notes.
- Bäumker, Brechtken, Heimes, Richter, 1997. *Practical Experiences with a High-Precision Stabilized Camera Platform Based on INS/(D)GPS*, *The First North American Symposium on Small Format Aerial Photography*.
- Hahn, H. and Klier, W., 1999. *Mathematical modeling and computer simulation of a camera attached to a platform inside an airplane (Part II: Spatial case)*. *RTS-Bericht RT-30, Part II*, Fachgebiet Regelungstechnik (Maschinenbau), Universität-Gh Kassel.
- Shortis, Robson, Beyer, 1998. *Principal Point Behaviour and Calibration Parameter Models for Kodak DCS Cameras*, *Photogrammetric Record*, 15(92), 20.
- Bäumker, Brechtken, Heimes, Richter, 1999. *Direkte Georeferenzierung mit dem Luftaufnahmesystem LEO, X*. *Internationale Geodätische Woche Obergurgl (Universität Innsbruck)*.
- Jacobsen, 2000. *Combined Bundle Block Adjustment Versus Direct Sensor Orientation*, *ASPRS Annual Convention*, Washington.